

# UV photonics integrated circuit for biomolecule detection with SiO<sub>2</sub> as a waveguide core on CaF<sub>2</sub>

X. Zheng,<sup>1,2</sup> N. Le Thomas,<sup>1,2</sup>

<sup>1</sup> Photonics Research Group, INTEC Department, Ghent University-imec, Technologiepark-Zwijnaarde, 9052 Ghent, Belgium

<sup>2</sup> Center for Nano- and Biophotonics, Ghent University, Belgium

*Optical biomedical sensors are envisioned to improve public health by monitoring body fluids of patients as for instance in intensive care units. They are however still suffering from either high cost or weak detection limits, which hinders them to have a real societal impact. Adopting photonic integrated circuits (PICs) for biosensors can save significant time and resource by realizing compact, scalable and reliable system. Up to now PICs have been developed mainly to operate in the visible, near infrared and mid infrared wavelength ranges leading to detection limits that are still too small. PICs operating in the UV and in particular in the UVC might be a game-changer considering that almost all biological molecules exhibit strong absorption in the UVC. Here we present photonics integrated circuits made of silicon dioxide thin layer on calcium fluoride substrate that are two material compatible with UV light down to a wavelength of 220nm. The optical losses of a single mode propagating in an air-top cladding waveguide are 5dB/cm and 3.5dB/cm at wavelengths of 266nm and 360nm, respectively, for a core waveguide thickness of 500nm and a width of 900 nm.*

## 1.Introduction

The success of silicon photonics for telecommunications has paved the way for the deployment of nano-scale photonics in various fields, including biological sensing [1]. Photonic chips benefit from significant compactness, and compatibility with standard microelectronics foundries, making them cost-effective solutions, in particular for label-free biosensors [1]. Unfortunately, silicon is unsuitable for application which requires ultraviolet (UV) light, a wavelength range, between 200nm and 400nm, for which biological molecules exhibit strong absorption (>20dB/cm) [2]. Less progress has been made for integrated devices operating in the UV range. Preliminary researches on single crystal aluminum nitride (AlN) grown on sapphire using metal-organic CVD have indicated a moderate waveguide-loss of 8 dB/cm at a wavelength of 390 nm [2]. But AlN suffers from high defect density and is restricted to 25 mm wafer. It has been shown that aluminum oxide (AlO<sub>x</sub>) enable light propagation in single mode waveguide with losses as low as loss 3 dB/cm at a wavelength of 371 nm [3]. But losses at 266 nm are still too high (>40dB/cm). A new waveguide core material compatible with technological processes used in standard foundries is still needed to develop photonic integrated circuits (PICs) operating in the UV range. Here, we show that silicon dioxide (SiO<sub>2</sub>) deposited via inductively coupled plasma chemical vapor deposition (ICP-CVD) on 4-inch calcium fluoride (CaF<sub>2</sub>) wafers is a relevant core waveguide material in the UV range: propagation loss of 5 dB/cm and 3.5 dB/cm are demonstrated at the wavelengths of 266 nm and 360 nm, respectively.

## 2. Waveguide properties

We have simulated the guided modes in SiO<sub>2</sub> waveguides with Lumerical to identify the parameter space for achieving a single-mode propagation. The thickness of SiO<sub>2</sub> core layer is designed to be 500 nm to inhibit higher-order TE modes. The evolution of the modal effective index with respect to the waveguide width is shown in Figure 1(a),(b). The cut-off width of the single mode operation is 1 μm and 1.9 μm for 266 nm and 360 nm, respectively. To make sure that the waveguide could be single mode for both 266 nm and 360 nm, a waveguide width of 0.9 μm has been chosen corresponding to a 10% margin from the cut-off width. For a single mode, the confinement ratio of the single mode in the waveguide core can be estimated from  $\int E_{core}(x, y) dx dy / \int E_{total}(x, y) dx dy$ . The TE modal electrical profile at a wavelength of 266 nm and 360 nm are shown in Figure 1(d), (e) with a confinement ratio of 0.82 and 0.61, respectively. The single mode is distributed more towards to the CaF<sub>2</sub> substrate at 360 nm (Figure 1(e)) compared to 266 nm (Figure 1(d)). Due to the low index contrast, the bending radius of the fully etched waveguide is on the order of hundreds of nanometers as simulated in Figure 1(f).

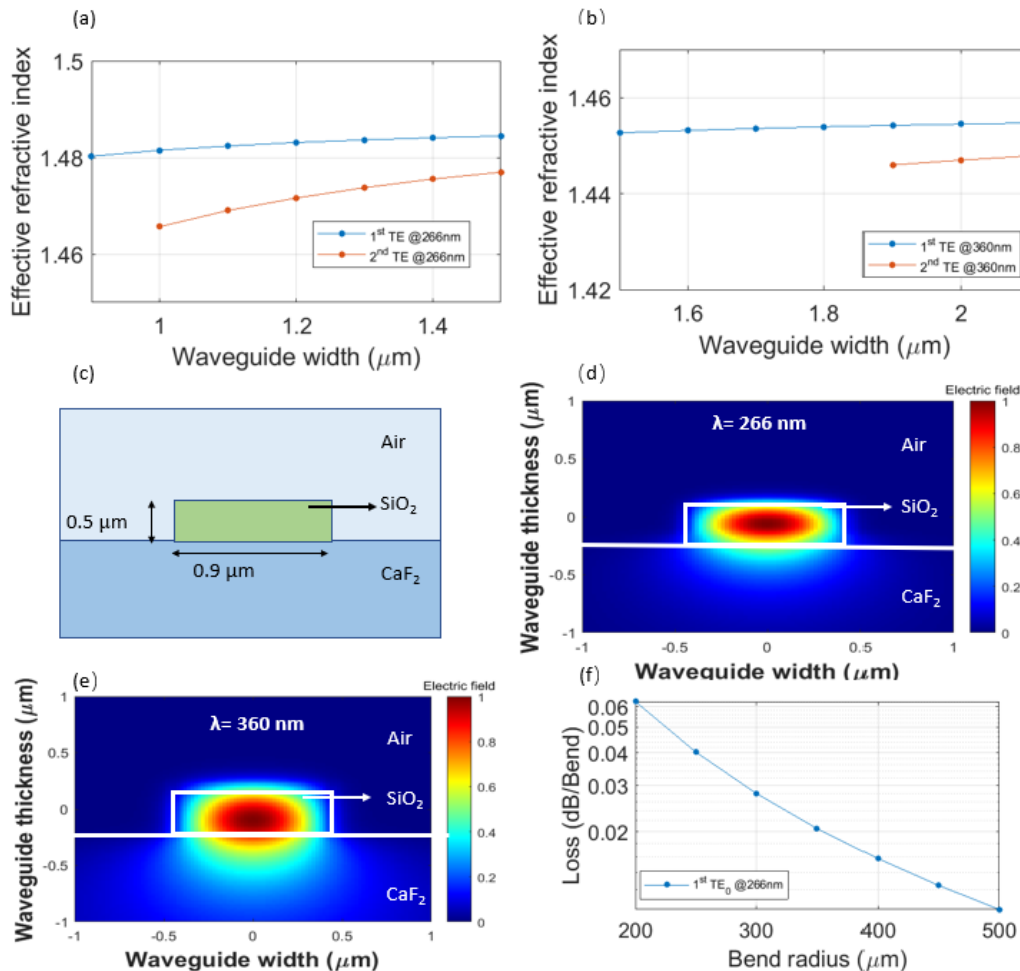


Figure 1: (a) Evolution of 1<sup>st</sup> and 2<sup>nd</sup> TE mode effective refractive index with respect to waveguide width at a wavelength of 266 nm and (b) 360 nm. (c) Schematic cross section and (d) simulated electric field distribution of the TE<sub>0</sub> mode in a waveguide core at a wavelength of 266 nm and (e) at 360 nm. The thickness and the width of the silicon dioxide wire waveguide are 500 nm and 900 nm, respectively. The thickness of the calcium fluoride substrate is 200 μm. (f) The simulated data of the losses per bend versus the bend radius at a wavelength of 266 nm.

### 3. Fabrication process

A cleaned CaF<sub>2</sub> wafers was used to deposit of a 500 nm SiO<sub>2</sub> layer via ICP-CVD. Then, an electron-beam resist (ARP6200.18) layer was spin-coated on top of the SiO<sub>2</sub>. It was patterned with electron beam lithography (EBL) to serve as a mask for etching the SiO<sub>2</sub> layer through inductively coupled plasma (ICP) dry etching. The waveguides were subsequently fabricated by fully etching the SiO<sub>2</sub> layer. Finally, the resist was removed by O<sub>2</sub> plasma, resulting in an air cladding at the top.

### 4. Experiments

We have determined the propagation losses of the guided mode by imaging the light scattered out of plane by residual roughness and quantifying the light intensity decay versus the propagation length at a wavelength of 266 nm and 360 nm, see Fig. 2. It is assumed that the sidewall roughness caused by dry etching process is randomly distributed along the waveguide. The propagation loss  $\alpha$  in dB/cm is expressed as  $\alpha = 10 \log_{10}(I_1/I_0)$  for a given the propagated length,  $I_0$  is the intensity of the scattered light at the input and  $I_1$  is the intensity of the scattered light after a given propagation length. A 300  $\mu\text{m}$  bend radius is chosen to minimize bend losses, see Fig. 1(f). The lack of uniformity of the scattered light in Fig. 2(b) is still under study. This might be caused by the inhomogeneity of the SiO<sub>2</sub> deposition or of the residual roughness introduced by the dry etching.

To extract the propagation losses,  $\alpha$ , we linearly fitted the scattered intensity versus the waveguide length as shown in Figure 2(d). The slope of the linear fit gives the propagation losses per unit length. The standard error was estimated based on the variance in four samples as well as multi sets of measurements with the same lengths.

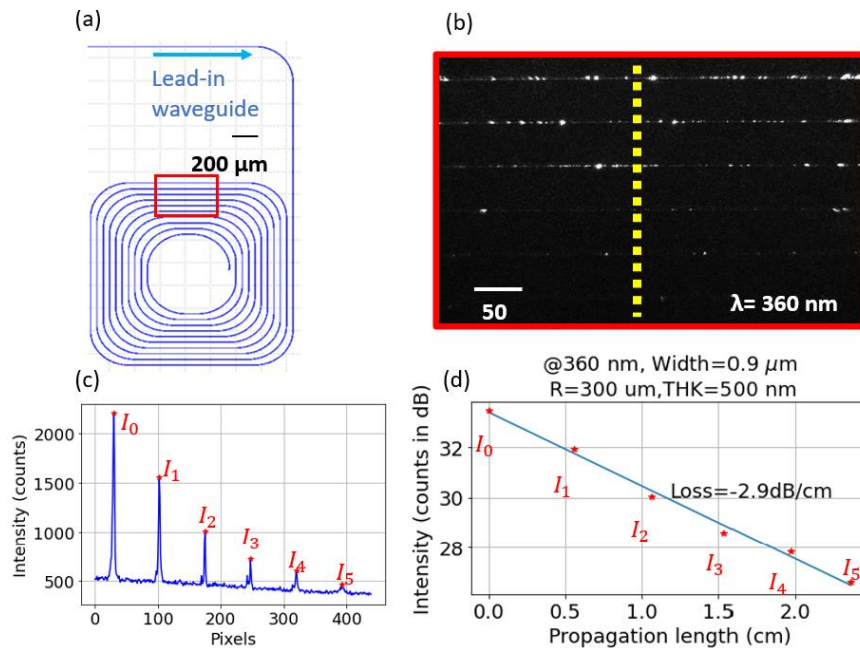


Figure 2: (a) A spiral layout shown in Klayout. (b) Microscopy image of the scattered light from a spiral waveguide (in the red rectangle in (a)) at a wavelength of 360nm. (c) A plot shows the average intensity profile of the scattered light along the dashed yellow line in (b). (d) Linear fitting between the scattering intensity versus waveguide length.

The propagation loss has been determined for several waveguide width, see Fig. 3. The propagation loss is estimated to be  $\sim 5$  dB/cm and 3.5 dB/cm at a wavelength of 266 nm and 360 nm respectively, for a single mode propagating in a waveguide of width 900 nm.

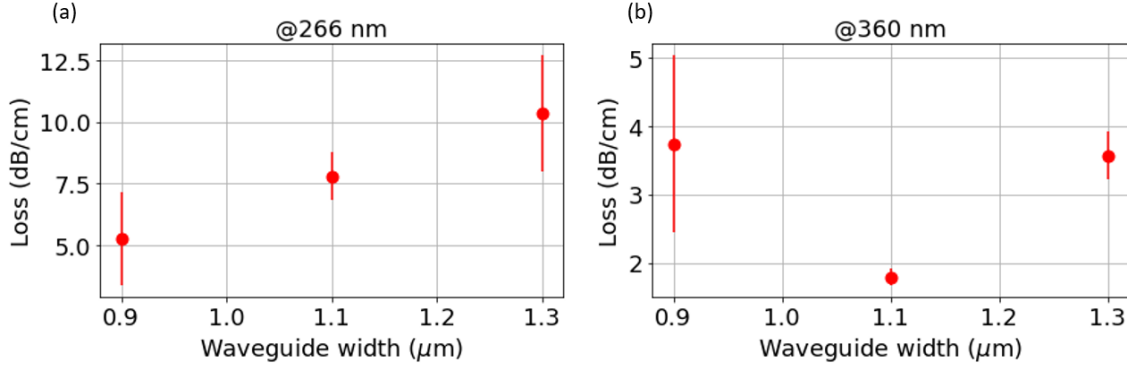


Figure 3: Relation between the propagation loss of the waveguide and the waveguide width at a wavelength of 266 nm (a) and 360 nm (b). The thickness of the waveguide is 500 nm.

Based on the simulation results presented in Figure 1(f), a loss of 0.03 dB per bend is expected for a bend radius of 300 μm, a waveguide core thickness of 500 nm and a width of 900 nm. Considering the 24 bends used in Fig 2(b), a total bending loss of 0.7 dB is expected, which is less than the margin of error of 2 dB. This significant standard error may be caused by the variation of SiO<sub>2</sub> deposition at different times or by the lack of uniformity of the scattered field in Fig. 2(b). Importantly, we observed an increase of the propagation losses at  $\lambda = 266$  nm when the waveguide width increases. This trend is not observed at  $\lambda = 360$  nm. It suggests that the absorption of the waveguide core is a limiting factor at  $\lambda = 260$  nm. At  $\lambda = 266$  nm, absorption dominates while at  $\lambda = 360$  nm, scattering loss might be more significant. To confirm our hypothesis, we will use water as a cladding instead of air in order to decrease the mode confinement and consequently the absorption loss. Note that water absorption is negligible at  $\lambda = 266$  nm as confirmed by a transmission experiment. If the propagation loss decreases for an increasing width, we will have reached a regime where the scattering loss are dominant at  $\lambda = 266$  nm.

## 5. Conclusion

Our waveguide made of SiO<sub>2</sub> deposited with ICP-CVD on a CaF<sub>2</sub> substrate have reached loss levels relevant for applications in UV range: 5 dB/cm and 3.5 dB/cm loss for a single mode waveguide at  $\lambda = 266$  nm and  $\lambda = 360$  nm, respectively. The absorption loss of the SiO<sub>2</sub> material is suspected as the main limiting factor at  $\lambda = 266$  nm. These achievements are promising to develop a new UVC platform including all basic building blocks of PICs.

## References

- [1] Iqbal, Muzammil, *et al.* "Label-free biosensor arrays based on silicon ring resonators and high-speed optical scanning instrumentation." IEEE Journal of selected topics in quantum electronics 16, no. 3 (2010): 654-661.

- [2] Sorace-Agaskar, *et al.* "Multi-layer integrated photonics from the ultraviolet to the infrared." In *Frontiers in Biological Detection: From Nanosensors to Systems X*, vol. 10510, pp. 36-45. SPIE, 2018.
- [3] Lin, Chupao. "UV photonic integrated circuits for label-free structured illumination microscopy and quantitative phase imaging." PhD diss., Ghent University, 2023.